

Classification of Parkinson's Disease Using the Frequency-Specific Changes of Resting Brain Activity

Jiaqi Tang, Runhan Zhang and Jiayi Pu
Keystone Academy, Beijing 101318, China

Keywords: Parkinson's Disease, Frequency-Specific Changes, Resting-State Functional Magnetic Resonance Imaging, Machine Learning, Classification.

Abstract: Resting state functional magnetic resonance imaging has become a widely used method for diagnosing Parkinson's disease. Nevertheless, machine-learning technology has not been used to better classify disease results from MRI signals. Here, the slow-frequency fluctuation amplitudes of patients and healthy controls are measured as input to the machine learning model. The features and classification capabilities of the machine learning model are respectively evaluated by the T-test and linear support vector machine. The signals from three frequency bands (Slow-5, 0.01-0.03 Hz; Slow-4, 0.03-0.08 Hz; conventional, 0.01-0.08 Hz) are analyzed. We found that in the classification of Parkinson's disease, Slow-4 signal provides more information than Slow-5, and its classification ability is comparable to traditional frequency bands. This study shows that machine-learning technology is a promising method of detecting abnormal areas and activities in Parkinson's disease, and multi-band data can give us more specific message.

1 INTRODUCTION

Parkinson's disease (PD) is a kind of neurodegenerative disease which mainly affects dopaminergic (dopamine-producing) neurons in the substantia nigra and basal ganglia (Blandini, 2000). Neurons in the substantia nigra produce the neurotransmitter dopamine, which regulates synaptic transmission and controls body movement. In PD patients, dopaminergic neurons in the substantia nigra gradually die. When 80% of dopaminergic neurons are lost, a variety of typical PD symptoms occur, including tremor, slow movement, stiffness, and balance problems (Surmeier, 2018). In addition to motor control, dopamine also plays a vital role in higher cognitive functions, including motivation, learning, and memory. In fact, dopamine deficiency is associated with many neurological and psychiatric diseases, such as Parkinson's disease, schizophrenia, depression, attention deficit/hyperactivity disorder (ADHD), and addiction (Burbulla, 2017). The decrease in dopamine levels mainly leads to abnormal brain activity in the basal ganglia network (Qian, 2017), motor system (Hu, 2019) and visual cortex (Meder, 2019; Spay, 2019). All of these can cause movement disorders and sensory and cognitive

symptoms, such as gearing, axial and limb stiffness, slow movement, stiffness, balance and tremor, and decreased sense of touch and smell (Surmeier, 2018).

Machine learning (ML) has been used in the study of the spatial patterns of abnormal cerebral activity areas in PD patients. It can be further divided into two phases. In the first phase, a model trained through data set is built, and in the second stage the classification ability from an independent test data set is evaluated. ML is an ideal new tool for clinical research because it can integrate complex imaging data into personalized diagnostic and prognostic indicators. Through comparison, it is clear that ML provides a more effective multivariate pattern to analyze the predictions for future observations than traditional univariate analysis. In addition, it produces independent P values that can be recorded in standard tests. The ML model has been applied to various data patterns for diagnosing PD, including handwriting patterns (Licarete, 2020; Wiviott, 2019), sports (Cherubini, 2014; Wahid, 2015), neural Image data (Choi, 2017), speech patterns (Sakar, 2013), cerebrospinal fluid (Maass, 2020), myocardial scintigraphy (Nuvoli, 2020), and serum (Váradi, 2019). ML also allows combining data from different experimental methods, including magnetic resonance

imaging (MRI) (Wang, 2017) and single photon emission computed tomography (SPECT) (Cherubini, 2014). Using the ML method, scientists have identified outstanding features that have traditionally not been used for clinical diagnosis of PD. In addition, they have ML to detect pre-clinical stage or atypical forms of disease and better understand the disease.

Resting functional magnetic resonance imaging (RS-fMRI) is a way of assessing regional interactions that occur at rest. It can be used to check PD on a macro scale. fMRI enables scientists to understand the neuronal activity in the body in PD (Meppelink, 2009). In addition, RS-fMRI enables scientists to understand how functionally specialized brain function areas change in comparison with structural MRI data.

The low frequency fluctuation amplitude (ALFF) derived from classic fMRI is a method to measure the total power within a given time in a typical frequency range (0.01–0.08 Hz), and has been proven to be an important indicator of regional spontaneous neurons activity. The different frequencies of neuronal oscillations may represent unique brain functions (Thut, 2012). In the current study, we will examine three frequency bands, Slow-5 (0.01–0.03 Hz), Slow-4 (0.03–0.08 Hz), and traditional frequency bands (0.01–0.08 Hz). Scientists found ALFF abnormalities in the auxiliary motor cortex, thalamus, putamen, and prefrontal cortex of PD patients (Skidmore, 2011).

In this study, we used Linear Support Vector Machine (LSVM) to classify PD patients and healthy controls (HC) according to slow 4, slow 5, and regular frequency bands. We found that Slow-4 shows superior classification ability than Slow 5 and is comparable to traditional bands.

2 MATERIALS AND METHODS

2.1 Background Information

The data for this study comes from an open source dataset used for fMRI experiments. The 161 right-handed participants were divided into two groups. One is composed of 72 PD patients, and the other is composed of 90 age- and gender-matched healthy controls (HC). All PD patients were diagnosed as the brain bank of the British Parkinson's Disease Association (Gibb, 1988). The exclusion criteria for PD patients include a Mini Mental State Examination (MMSE) score <24, acute physical diseases, mainly neurological diseases and other mental diseases. MRI examination revealed no obvious abnormalities,

history of mental illness, or neurological disease. Actual "on" state which includes Hoehn and Yahr staging scale (H&Y) (Hoehn, 1998), Unified Parkinson's Disease Rating Scale Exercise Part III (UPDRS III) (Vassar, 2012) and global Cognitive function (Folstein, 1975) is used to evaluate the clinical indicators of each PD patient.

2.2 MRI Data Acquisition

A 3.0 Tesla MR system (Discovery MR750, General Electric, Milwaukee, WI, USA) was used to retrieve magnetic resonance (MR) images. It acquires RS-fMRI data through gradient echo planar imaging (GRE-EPI) sequence with the following parameters: repetition time (TR) = 2000 ms, echo time (TE) = 30 ms, flip angle = 90°, matrix size = 64 × 64, field of view (FOV) = 220 × 220 mm², thickness/gap = 3.5 mm / 0.6 mm, number of slices = 31. They obtained the data of 140 participants' brain volumes. During the experiment, the participants were asked to close their eyes, don't think about anything and don't fall asleep. In order to obtain high-resolution structural images for standardization purposes, we applied a T1-weighted fluid attenuation inversion recovery (FLAIR) sequence with the following parameters: TR = 2530 ms, TE = 3.34 ms, flip angle = 7°, matrix = 256 × 256, FOV = 256 × 256 mm², thickness = 1 mm, no gap, number of slices = 196.

2.3 Image Processing

FMRIB software library (FSL: <http://www.fmrib.ox.ac.uk/fsl>, version 5.0) and functional NeuroImaging analysis (AFNI: <http://afni.nimh.nih.gov/afni>, version 2011_12_21_1014) It is used to perform standard preprocessing steps, including motion correction, joint registration, segmentation and normalization. Remove irrelevant noises that cause white matter, ventricular signals, global signals, and motion parameters to obtain fMRI signals for each voxel. No spatial smoothing was performed in this study. In order to determine the frequency-specific fMRI profile to classify PD classification, the voxel ALFF graph of the three frequency intervals (slow 5, 0.01–0.03 Hz and slow 4, 0.03–0.08 Hz and regular, 0.01–0.08 Hz) is used REST The filter function provided in the toolbox is calculated (Yang, 2007; Song, 2014). We use the code in the Connectome Computation System to determine the frequency band (Xu, 2015).

2.4 Feature Extraction, Feature Selection and Classification

The automatic anatomical labeling (AAL) template image is used to estimate the average ALFF value of each subject and extract the functional magnetic resonance spectrum features of ML (Tzourio-Mazoyer, 2002). Ninety brain regions were selected. Therefore, we used the three frequency bands respectively (slow 5, slow 4, or traditional) to obtain a matrix of 90 features for 161 subjects. Moreover, in order to check the effect of the method on the basis of the structure atlas on our results, we performed feature extraction based on the Power-264 atlas (Power, 2011) and the Yeo-17 network (Thomas, 2011). Compared to the classification performance of slow 5, slow 4, and traditional frequency band combinations, we concatenate the ALFF values of slow 5 and slow 4 to generate a single original feature vector for each topic (Wee, 2012).

Implemented a feature selection method to achieve high accuracy, study the most distinguishing features, and avoid overfitting in the final classifier training. According to previous research, two-sample t-test was chosen for the feature selection method (Cui, 2016). The outer loop is used to evaluate classification performance, and the inner loop is used to select the best subset of features. The classification performance of these two loops is evaluated by linear support vector machine (LSVM), which is one of the most commonly used supervised ML methods. Matlab's LIBSVM toolbox is used to perform LSVM classification (Chang, 2011). The penalty factor C is set to 1 (Cui, 2016). According to the LSVM score, participants with positive scores are classified as HC, and those with negative scores are classified as PD.

The detailed steps are as follows (Figure 1). (1) Randomly select one subject from the entire data set (N subjects) as the test subject, and leave the rest (N-1 subjects) as the training set for each LOOCV. (2) Repeat the inner LOOCV in each outer LOOCV fold, and obtain N-2 subjects as the training subset of each inner LOOCV. (3) Introduce the training subset of each internal LOOCV (N-2 subjects) into feature selection. In this study, we perform a two-sample t-test for each feature and calculate the P value. Feature selection is processed on the basis of a P threshold from 0 to 1, with an interval of 0.01. Include and exclude features below and above the P threshold, respectively. The feature selection procedure is repeated N-1 times for each P threshold, which results in the accuracy of internal cross-validation. Then we define the optimal P threshold is defined as the P value with the highest internal cross-validation

accuracy. This threshold is used for the final classifier training in the external LOOCV and obtain the final cross-validation accuracy score (Wee, 2012).

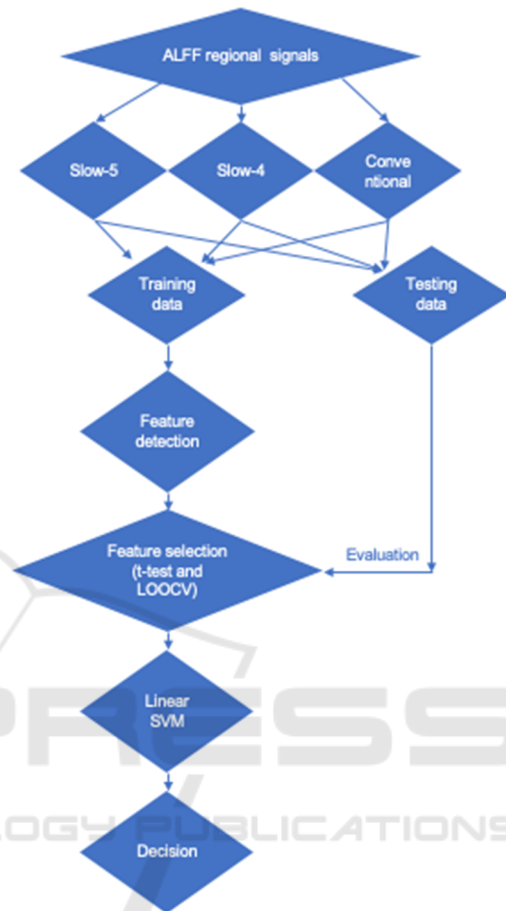


Figure 1: Flow chart of data processing and ML modelling.

2.5 Evaluation of the Classification Power of Various Indices

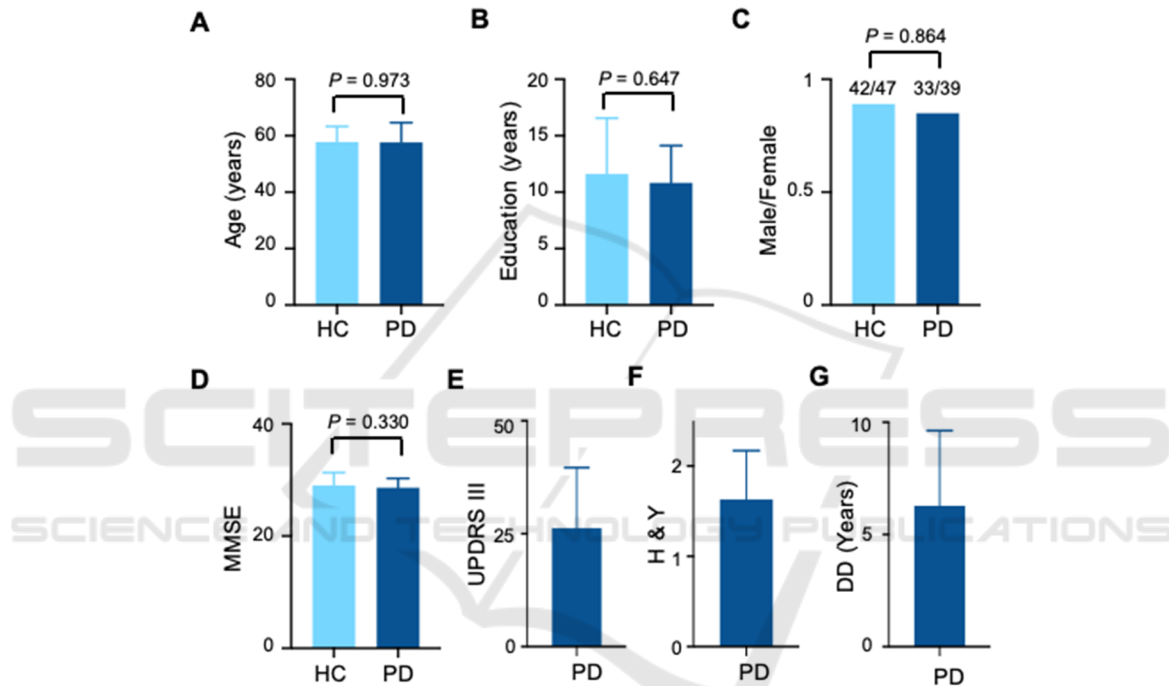
We use accuracy, sensitivity, and specificity values to assess the classification ability of specific ALFF methods at different frequencies. In addition, receiver operating characteristics (ROC) and area under ROC (AUC) are also used to evaluate the classification performance of specific fMRI features in different frequency bands, too. In addition, 1000 permutation tests were performed to assess whether the figure of the AUC and accuracy were significantly higher than the random value. In addition, in order to compare the classification performance of the multi-band (Slow-5 and Slow-4) with that of the single-band (Slow-5, Slow-4 or traditional), we calculated the accuracy difference and the AUC difference between them. For

nonparametric statistical tests, the P-value for accuracy or AUC (or its difference) is calculated by dividing by the number of permutations that show the actual value (or its difference) higher than the real sample.

3 RESULTS

3.1 Basic Information

We did not find any significant differences in the age (PD: 57.7 ± 7.0 , HC: 57.7 ± 5.6 , $P = 0.97$, two-sample unpaired two-tailed t-test, $N = 72, 89$, respectively), education level (PD: 10.8 ± 3.3 , HC: 11.6 ± 5.0 , $P = 0.65$, two-sample unpaired two-tailed t-test, $N = 72, 89$, respectively), sex (PD: 33/39, HC: 42/47, $P = 0.86$, Fisher's exact test, $N = 72, 89$, respectively), or MMSE scores (PD: 28.6 ± 1.7 , HC: 29.0 ± 2.3 , $P = 0.33$, two-sample unpaired two-tailed t-test, $N = 72, 89$, respectively) between PD patients and HCs. The UPDRS III score, H&Y score, and disease duration for PD patients were 26.2 ± 13.4 , 1.6 ± 0.5 , and 6.3 ± 3.4 years, respectively (Figure 2).



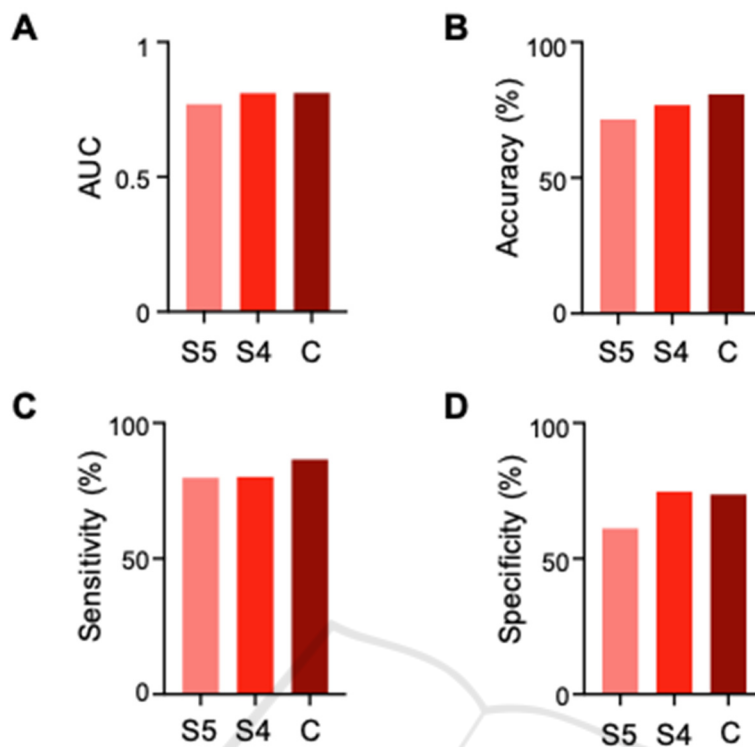
A. Distribution of ages of HC and PD. $P = 0.973$, two-sample unpaired two-tailed t-test, $n = 89$ and 72 . B. Distribution of education years. $P = 0.647$, two-sample unpaired two-tailed t-test, $n = 89$ and 72 . C. Distribution of Male/Female ratios. $P = 0.854$, Fisher's exact test, $n = 89$ and 72 . D. Distribution of MMSE values. $P = 0.330$, two-sample unpaired two-tailed t-test, $n = 89$ and 72 . E. Distribution of UPDRS III values. $n = 72$. F. Distribution of H & Y values. $n = 72$. G. Distribution of disease duration (DD). $n = 72$.

Figure 2: Basic information of health controls (HC) and PD patients.

3.2 Classification Performance

This study used three frequency bands, namely slow 5, slow 4 and regular frequency bands. The classification is then determined by the linear support vector machine (LSVM), a machine learning model based on these bands. We further evaluated the performance of the model (ie, AUC, accuracy, sensitivity, and specificity). According to the AUC value, we found that the performance of the models based on Slow-5, Slow-4, and Conventional

frequency bands are 0.77, 0.81, and 0.84, respectively; according to the Accuracy values, they are 71.4, 76.8, and 79.5; according to the Sensitivity values, they are 61.1, 74.7, and 73.6; According to the specificity values, they were 79.8, 80.2 and 86.5 (Figure 3). These results show that classification based on Slow-4 signal is better than classification based on Slow-5 signal. In addition, the performance of models based on Slow-4 signals is mostly comparable to traditional frequency bands. Together, we found that Slow-4 can be used as a diagnostic criteria for PD patients to classify HC.



A. Comparison of AUC values among group S5, S4, and C. B. Comparison of Accuracy values (%) among group S5, S4, and C. C. Comparison of Sensitivity values (%) among group S5, S4, and C. D. Comparison of Specificity values (%) among group S5, S4, and C. LSVM, linear support vector machine; Slow-5 (S5), 0.01–0.03 Hz; Slow-4 (S4), 0.03–0.08 Hz; Conventional (C), 0.01–0.08 Hz; AUC, area under curve.

Figure 3: The results of the LSVM classifier with a single or combined features.

4 DISCUSSION

In the study, we used ML methods and multivariate analysis to analyze the multi-frequency signals in the brain and found two main findings. First of all, the classification performance of all frequency band-based schemes is significantly higher than that of random schemes, indicating that all frequency bands have good diagnostic capabilities. Secondly, through comparing the classification performance of Slow-5 and Slow-4, we find the latter has more information in PD classification than Slow-5.

Using LSVM to compare the classification performance of each pair of schemes based on frequency bins, we found that slow 4 signals (0.03-0.08 Hz) provide more information on the pathogenesis of PD. In addition, the results of the ML method show that compared with the traditional frequency band, the Slow-4 signal shows almost the same classification performance. This shows that a specific frequency interval can provide the most information for PD classification.

Although the traditional method shows classification performance comparable to multi-band fMRI data processing, it fails to detect abnormal activities in the lateral parietal cortex (Blandini, 2000; Tumati, 2019). Previous researches have shown that this dysfunction is relevant to the pathogenesis of PD (Tumati, 2019). In addition, the classification performance of Slow-4 is superior to the traditional frequency band (0.01-0.08 Hz) in distinguishing the frozen and non-frozen gait of PD patients (Hu, 2017). In summary, the results show that multiple frequency bands can provide more information for PD detection and classification.

5 CONCLUSION

In summary, here we established a ML framework based on specific frequency bands in the ALFF signals from the RS-fMRI data for the diagnosis of PD. The results suggested the information from a specific band (Slow-4) can provide more information

than any other frequency interval and is comparable to the conventional wide-band frequency signals. These data highlight the classification power of ML approaches in the classification of PD by detecting subtle and complex changes in the ALFF signals. This study will shed light on future research on the diagnosis and treatment for PD patients.

REFERENCES

- Blandini, F, G Nappi, C Tassorelli, and E Martignoni. 2000. "Functional Changes of the Basal Ganglia Circuitry in Parkinson's Disease." *Progress in Neurobiology* 62 (1): 63–88. [https://doi.org/10.1016/s0301-0082\(99\)00067-2](https://doi.org/10.1016/s0301-0082(99)00067-2).
- Burbulla, Lena F, Pingping Song, Joseph R Mazzulli, Enrico Zampese, Yvette C Wong, Sohee Jeon, David P Santos, et al. 2017. "Dopamine Oxidation Mediates Mitochondrial and Lysosomal Dysfunction in Parkinson's Disease." *Science* 357 (6357): 1255–61. <https://doi.org/10.1126/science.aam9080>.
- Cherubini, Andrea, Rita Nisticó, Fabiana Novellino, Maria Salsone, Salvatore Nigro, Giulia Donzuso, and Aldo Quattrone. 2014. "Magnetic Resonance Support Vector Machine Discriminates Essential Tremor with Rest Tremor from Tremor-Dominant Parkinson Disease." *Movement Disorders* 29 (9): 1216–19. <https://doi.org/10.1002/mds.25869>.
- Choi, Hongyoon, Seunggyun Ha, Hyung Jun Im, Sun Ha Paek, and Dong Soo Lee. 2017. "Refining Diagnosis of Parkinson's Disease with Deep Learning-Based Interpretation of Dopamine Transporter Imaging." *NeuroImage: Clinical* 16: 586–94. <https://doi.org/10.1016/j.nicl.2017.09.010>.
- Cui, Zaixu, Zhichao Xia, Mengmeng Su, Hua Shu, and Gaolang Gong. 2016. "Disrupted White Matter Connectivity Underlying Developmental Dyslexia: A Machine Learning Approach." *Human Brain Mapping* 37 (4): 1443–58. <https://doi.org/10.1002/hbm.23112>.
- Chang, Luke J., Alec Smith, Martin Dufwenberg, and Alan G. Sanfey. 2011. "Triangulating the Neural, Psychological, and Economic Bases of Guilt Aversion." *Neuron* 70 (3): 560–72. <https://doi.org/10.1016/j.neuron.2011.02.056>.
- Folstein, Marshal F, Susan E Folstein, and Paul R McHugh. 1975. "Mini-Mental State." *Journal of Psychiatric Research* 12 (3): 189–98. [https://doi.org/10.1016/0022-3956\(75\)90026-6](https://doi.org/10.1016/0022-3956(75)90026-6).
- Gibb, W R, and A J Lees. 1988. "The Relevance of the Lewy Body to the Pathogenesis of Idiopathic Parkinson's Disease." *Journal of Neurology, Neurosurgery & Psychiatry* 51 (6): 745–52. <https://doi.org/10.1136/jnnp.51.6.745>.
- Hoehn, M M, and M D Yahr. 1988. "Parkinsonism: Onset, Progression, and Mortality." *Neurology* 50 (2): 318. <https://doi.org/10.1212/WNL.50.2.318>.
- Hu, Xiaofei, Yuchao Jiang, Xiaomei Jiang, Jiuquan Zhang, Minglong Liang, Jing Li, Yanling Zhang, Dezhong Yao, Cheng Luo, and Jian Wang. 2017. "Altered Functional Connectivity Density in Subtypes of Parkinson's Disease." *Frontiers in Human Neuroscience* 11 (September). <https://doi.org/10.3389/fnhum.2017.00458>.
- Hu, Hongping, Yangyang Li, Yanping Bai, Juping Zhang, and Maoxing Liu. 2019. "The Improved Antlion Optimizer and Artificial Neural Network for Chinese Influenza Prediction." *Complexity* 2019 (August): 1–12. <https://doi.org/10.1155/2019/1480392>.
- Licarete, Emilia, Valentin Florian Rauca, Lavinia Luput, Denise Drotar, Ioana Stejerean, Laura Patras, Bogdan Dume, et al. 2020. "Overcoming Intrinsic Doxorubicin Resistance in Melanoma by Anti-Angiogenic and Anti-Metastatic Effects of Liposomal Prednisolone Phosphate on Tumor Microenvironment." *International Journal of Molecular Sciences* 21 (8): 2968. <https://doi.org/10.3390/ijms21082968>.
- Maass, Fabian, Bernhard Michalke, Desiree Willkommen, Andreas Leha, Claudia Schulte, Lars Tönges, Brit Mollenhauer, et al. 2020. "Elemental Fingerprint: Reassessment of a Cerebrospinal Fluid Biomarker for Parkinson's Disease." *Neurobiology of Disease* 134 (February): 104677. <https://doi.org/10.1016/j.nbd.2019.104677>.
- Meder, David, Damian Marc Herz, James Benedict Rowe, Stéphane Lehericy, and Hartwig Roman Siebner. 2019. "The Role of Dopamine in the Brain - Lessons Learned from Parkinson's Disease." *NeuroImage* 190 (April): 79–93. <https://doi.org/10.1016/j.neuroimage.2018.11.021>.
- Meppelink, A. M., B. M. de Jong, R. Renken, K. L. Leenders, F. W. Cornelissen, and T. van Laar. 2009. "Impaired Visual Processing Preceding Image Recognition in Parkinson's Disease Patients with Visual Hallucinations." *Brain* 132 (11): 2980–93. <https://doi.org/10.1093/brain/awp223>.
- Nuvoli, Susanna, Angela Spanu, Mario Luca Fravolini, Francesco Bianconi, Silvia Cascianelli, Giuseppe Madeddu, and Barbara Palumbo. 2020. "[123I] Metaiodobenzylguanidine (MIBG) Cardiac Scintigraphy and Automated Classification Techniques in Parkinsonian Disorders." *Molecular Imaging and Biology* 22 (3): 703–10. <https://doi.org/10.1007/s11307-019-01406-6>.
- Power, Jonathan D, Alexander L Cohen, Steven M Nelson, Gagan S Wig, Kelly Anne Barnes, Jessica A Church, Alecia C Vogel, et al. 2011. "Functional Network Organization of the Human Brain." *Neuron* 72 (4): 665–78. <https://doi.org/10.1016/j.neuron.2011.09.006>.
- Qian, Long, Yi Zhang, Li Zheng, Xuemei Fu, Weiguo Liu, Yuqing Shang, Yaoyu Zhang, et al. 2017. "Frequency Specific Brain Networks in Parkinson's Disease and Comorbid Depression." *Brain Imaging and Behavior* 11 (1): 224–39. <https://doi.org/10.1007/s11682-016-9514-9>.
- Sakar, Betül Erdogdu, M Erdem Isenkul, C Okan Sakar, Ahmet Sertbas, Fikret Gurgun, Sakir Delil, Hulya Apaydin, and Olcay Kursun. 2013. "Collection and Analysis of a Parkinson Speech Dataset With Multiple

- Types of Sound Recordings.” *IEEE Journal of Biomedical and Health Informatics* 17 (4): 828–34. <https://doi.org/10.1109/JBHI.2013.2245674>.
- Skidmore, F.M., M. Yang, L. Baxter, K.M. von Deneen, J. Collingwood, G. He, K. White, et al. 2013. “Reliability Analysis of the Resting State Can Sensitively and Specifically Identify the Presence of Parkinson Disease.” *NeuroImage* 75 (July): 249–61. <https://doi.org/10.1016/j.neuroimage.2011.06.056>.
- Song, Xiaopeng, Yi Zhang, and Yijun Liu. 2014. “Frequency Specificity of Regional Homogeneity in the Resting-State Human Brain.” Edited by Fa-Hsuan Lin. *PLoS ONE* 9 (1): e86818. <https://doi.org/10.1371/journal.pone.0086818>.
- Spay, Charlotte, Garance Meyer, Marie-Laure Welter, Brian Lau, Philippe Boulinguez, and Bénédicte Ballanger. 2019. “Functional Imaging Correlates of Akinesia in Parkinson’s Disease: Still Open Issues.” *NeuroImage: Clinical* 21: 101644. <https://doi.org/10.1016/j.nicl.2018.101644>.
- Surmeier, Dalton James. 2018. “Determinants of Dopaminergic Neuron Loss in Parkinson’s Disease.” *The FEBS Journal* 285 (19): 3657–68. <https://doi.org/10.1111/febs.14607>.
- Thomas Yeo, B T, Fenna M Krienen, Jorge Sepulcre, Mert R Sabuncu, Danial Lashkari, Marisa Hollinshead, Joshua L Roffman, et al. 2011. “The Organization of the Human Cerebral Cortex Estimated by Intrinsic Functional Connectivity.” *Journal of Neurophysiology* 106 (3): 1125–65. <https://doi.org/10.1152/jn.00338.2011>.
- Thut, Gregor, Carlo Miniussi, and Joachim Gross. 2012. “The Functional Importance of Rhythmic Activity in the Brain.” *Current Biology: CB* 22 (16): R658–63. <https://doi.org/10.1016/j.cub.2012.06.061>.
- Tzourio-Mazoyer, N, B Landeau, D Papathanassiou, F Crivello, O Etard, N Delcroix, B Mazoyer, and M Joliot. 2002. “Automated Anatomical Labeling of Activations in SPM Using a Macroscopic Anatomical Parcellation of the MNI MRI Single-Subject Brain.” *NeuroImage* 15 (1): 273–89. <https://doi.org/10.1006/nimg.2001.0978>.
- Tumati, S, S Martens, B M de Jong, and A Aleman. 2019. “Lateral Parietal Cortex in the Generation of Behavior: Implications for Apathy.” *Progress in Neurobiology* 175 (April): 20–34. <https://doi.org/10.1016/j.pneurobio.2018.12.003>.
- Váradi, Csaba, Károly Nehéz, Olivér Hornyák, Béla Viskolcz, and Jonathan Bones. 2019. “Serum N-Glycosylation in Parkinson’s Disease: A Novel Approach for Potential Alterations.” *Molecules* 24 (12): 2220. <https://doi.org/10.3390/molecules24122220>.
- Vassar, Stefanie D, Yvette M Bordelon, Ron D Hays, Natalie Diaz, Rebecca Rausch, Cherry Mao, and Barbara G Vickrey. 2012. “Confirmatory Factor Analysis of the Motor Unified Parkinson’s Disease Rating Scale.” *Parkinson’s Disease* 2012: 1–10. <https://doi.org/10.1155/2012/719167>.
- Wiviott, Stephen D, Itamar Raz, Marc P Bonaca, Ofri Mosenzon, Eri T Kato, Avivit Cahn, Michael G Silverman, et al. 2019. “Dapagliflozin and Cardiovascular Outcomes in Type 2 Diabetes.” *New England Journal of Medicine* 380 (4): 347–57. <https://doi.org/10.1056/NEJMoa1812389>.
- Wahid, Ferdous, Rezaul K Begg, Chris J Hass, Saman Halgamuge, and David C Ackland. 2015. “Classification of Parkinson’s Disease Gait Using Spatial-Temporal Gait Features.” *IEEE Journal of Biomedical and Health Informatics* 19 (6): 1794–1802. <https://doi.org/10.1109/JBHI.2015.2450232>.
- Wang, Zhengxia, Xiaofeng Zhu, Ehsan Adeli, Yingying Zhu, Feiping Nie, Brent Munsell, and Guorong Wu. 2017. “Multi-Modal Classification of Neurodegenerative Disease by Progressive Graph-Based Transductive Learning.” *Medical Image Analysis* 39 (July): 218–30. <https://doi.org/10.1016/j.media.2017.05.003>.
- Wee, Chong-Yaw, Pew-Thian Yap, Kevin Denny, Jeffrey N Browndyke, Guy G Potter, Kathleen A Welsh-Bohmer, Lihong Wang, and Dinggang Shen. 2012. “Resting-State Multi-Spectrum Functional Connectivity Networks for Identification of MCI Patients.” Edited by Yong He. *PLoS ONE* 7 (5): e37828. <https://doi.org/10.1371/journal.pone.0037828>.
- Xu, Ting, Zhi Yang, Lili Jiang, Xiu-Xia Xing, and Xi-Nian Zuo. 2015. “A Connectome Computation System for Discovery Science of Brain.” *Science Bulletin* 60 (1): 86–95. <https://doi.org/10.1007/s11434-014-0698-3>.
- Yang, Hong, Xiang-Yu Long, Yihong Yang, Hao Yan, Chao-Zhe Zhu, Xiang-Ping Zhou, Yu-Feng Zang, and Qi-Yong Gong. 2007. “Amplitude of Low Frequency Fluctuation within Visual Areas Revealed by Resting-State Functional MRI.” *NeuroImage* 36 (1): 144–52. <https://doi.org/10.1016/j.neuroimage.2007.01.054>.